Structural Effects on the Pb(110) Surface between 160 and 580 K Observed by Low-Energy Ion Scattering

S. Speller, M. Schleberger, A. Niehof, and W. Heiland
Fachbereich Physik, Universität Osnabrück, D-4500 Osnabrück, Germany
(Received 9 August 1991; revised manuscript received 6 February 1992)

Low-energy ion scattering and surface channeling is used to study structural changes of the Pb(110) surface. There is experimental evidence for point defects (vacancies) formed at 160 K, step and/or adatom formation at 270 K, and liquidlike surface phase at 580 K. In the neutral impact collision ion scattering spectrometry mode a thermal expansion of the [1$\bar{1}$0] surface lattice constant of 10% at 400 K is measured.

PACS numbers: 68.35.-p, 61.80.Mk, 79.20.Rf

The Pb(110) surface has been found to show surface-induced melting [1]. Since then other Pb $\{hkl\}$ surfaces have been studied by a variety of experimental techniques and theories [2,3]. For Pb(110) the melting proper is preceded by a premelting regime between 450 and 580 K [4]. In the premelting region some surface layers exhibit disorder which involves already positional (i.e., liquidlike) disorder. Up to 450 K all observations indicate enhanced thermal vibrations [1–6]. LEED (low-energy electron diffraction) studies established a roughening transition at about 400 K [3,7]. The roughening is not detected by MEIS (medium-energy ion scattering), but there is agreement that around 575 K roughness changes into liquidlike behavior as concluded from the MEIS and XPD (x-ray photoelectron diffraction) results [8–10]. LEED and MEIS experiments [8,11] showed an anisotropy of the surface disordering process which was not confirmed by other LEED experiments [3]. The roughness is understood as a step formation process. The length of the steps depends on the temperature, i.e., decreases with increasing temperatures, whereas the number of steps increases with increasing temperatures [3].

In the present work we present results from three different low-energy ion scattering methods: surface blocking, surface channeling, and NICISS (neutral impact collision ion scattering spectrometry) [12,13]. We find general agreement with some of the previous findings, but somewhat more specific, i.e., saturated disorder at 480 K, liquidlike behavior reached at 580 K. A new result is the evidence for the formation of vacancies in the [1$\bar{1}$0] surface chains of Pb(110) at temperatures as low as 160 K. A "good" (1×1) surface is only found at about 160 K, i.e., with a surface blocking pattern comparable in quality with those of Pt(110) or Au(110) [13,14]. Another new result is the anomalous expansion of the [1$\bar{1}$0] lattice constant.

The experimental setup has been described previously [15,16]. A UHV system with a magnetically analyzed ion beam, LEED system, electrostatic energy analyzer (ESA), time-of-flight system (TOF), and position sensitive detector (PSD) is used. For the present study we use 2 keV Ne^+ only, except for surface chemical analysis with the ESA, where He^+ is used also [ISS (ion scattering spectroscopy)] [12]. The Ne beam is also used for sputter cleaning for several days initially, with intermitting heating cycles and changing of the azimuthal angle. The angle of incidence is varied between 30° and 5° (glancing angle). After satisfactory cleanliness (ISS) and good surface periodicity (LEED) have been achieved only the lowest impact angles are used for further cleaning. The Pb crystal is mounted in a Cu crucible free of mechanical stress.

Figure 1 shows surface blocking patterns as a function of the temperatures measured with 2 keV Ne^+ incident at a grazing angle of 11°. The TOF detector at 165° is used to detect the backscattered Ne particles. The minima at [1$\bar{1}$0], [1$\bar{1}$1], [1$\bar{1}$2], [1$\bar{1}$4], and [001] are typical for a fcc (110) (1×1) surface structure [14]. The complete disappearence of these channeling minima has not been seen before. Since ion scattering in this mode is a "short-range-order technique," this flattening can only be due to a liquidlike surface phase formed at 580 K. Since single and double scattering events [12] contribute to the intensity, we can estimate trajectory lengths to

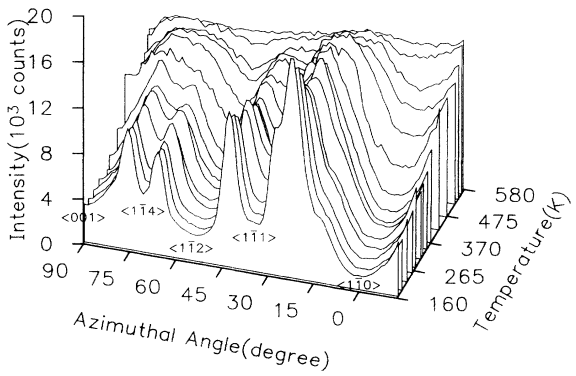

FIG. 1. Surface blocking patterns, I vs ϕ, for 2 keV Ne^+ scattered from Pb(110) at temperatures between 160 and 580 K. The angle of incidence (glancing angle) is 11°; the scattering angle is 165°.

be below 10 Å [17]. When comparing the measured blocking pattern with the calculations we find that above 400 K the formation of the minima is strongly influenced by steps along [1$\bar{1}$0] and [1$\bar{1}$2] (details to be published [17]). This finding suggests "fish-scale-like" structures as observed on Au(110) by STM (scanning tunneling microscopy) [18]. When inspecting the intensities of the minima in the azimuthal pattern (Fig. 1) we find a continuous increase of the minimal intensity. This increase is due to adatoms and/or steps, as concluded from comparable findings from Au(110) and Ir(110) [19]. The minimum yield data at 160 K are evidence for the existence of steps along [1$\bar{1}$0] which cause the blocking of all other channels. At about RT the number of steps increases up to about 400 K where the yields for [1$\bar{1}$1] and [1$\bar{1}$4] saturate. The yields of [1$\bar{1}$0], [1$\bar{1}$2], and [001] increase continuously, indicating that steps exist also along [1$\bar{1}$2] and that at higher temperature the steps decay again [3]. Detailed calculations will be published [17]. Finally the intensities merge at 580 K, clear evidence for a liquidlike layer.

The ion scattering experiment in the NICISS mode [12,13] (Fig. 2) shows the presence of vacancies in the [1$\bar{1}$0] surface chains even at 160 K. The evaluation of the I vs ψ data (glancing angle of incidence) is straightforward, the curves shown are calculated using a two-atom scattering model. The model is based on the classical shadow cone behind an atom [20]. By varying the angle of incidence a second atom behind the leading atom is used as a detector for the shadow cone cast by the leading atom. Parameters entering into the calculation are the interaction potential, the surface thermal vibrations (here corresponding to a Debye temperature $\Theta_s = 73$ K), and the surface lattice constant (3.5 Å for a perfect [1$\bar{1}$0] chain). The main contribution to the thermal vibrations are the displacements perpendicular to the surface [19]. The critical angles of 22.7° and 14.2° found in the experiment give values of 3.5 and 6.4 Å for the distance between the two atoms neighboring the vacancy. The reduction of the value for the vacancy may be due to an actual relaxation or an anharmonic potential for the atoms at the end of [1$\bar{1}$0] chains. At room temperature the experimental result already deviates strongly from the calculated result for a perfect chain. This discrepancy is solved by assuming an anomalous expansion of the lattice constant which causes the observed shift of the critical angle (Table I). Table I summarizes the results of the [1$\bar{1}$0] and of the [1$\bar{1}$2] measurements. No change of $a_{[1\bar{1}2]}$ is found. The thermal amplitudes are identical for the two directions and they follow the Debye law within the temperature range of 160 to 400 K. The quality of the "fit" between calculation and experiment can be judged from the mean-square deviation given in Table I. The number of vacancies and the [1$\bar{1}$0] lattice constant expansion are averages of the top two "visible" layers of the surface including step edges. Even a pair of adatoms in a [1$\bar{1}$0] trough will contribute to a [1$\bar{1}$0]. The theory [21] predicts vacancies in the second layer mainly in qualitative agreement with our findings. It is sensible to assume that vacancies exist in step edges (link sites [18], and other STM studies); these sites are not taken into account theoretically [21].

A qualitative measure of the disorder as a function of temperature is obtained from the surface channeling experiment (Fig. 3). At low temperatures we find the expected "half moon" shaped intensity distributions, e.g.,

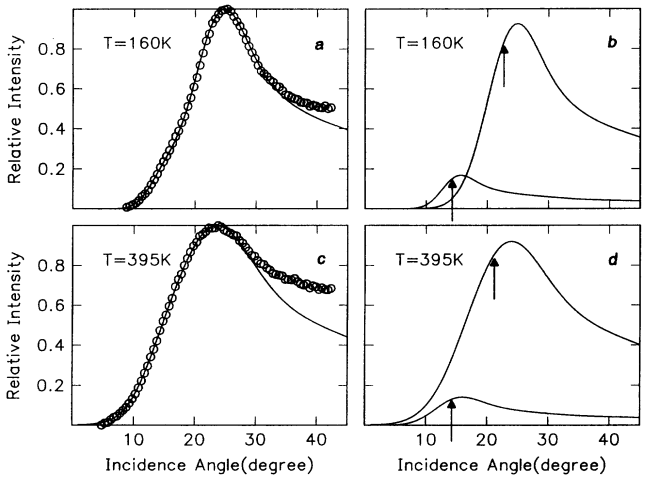

FIG. 2. Intensity vs glancing angle of incidence, I vs ψ, along [1$\bar{1}$0] at 160 and 395 K. Circles are the experimental intensity values [(a),(c)]. The lines are calculated using the two-atom shadow cone model. The small peak is calculated for single vacancies, the large peak for a perfect [1$\bar{1}$0] chain [(b),(d)]. The arrows mark the critical angles from which the surface lattice constants are calculated. (a) and (c) show the experiment and the sum of the calculated intensities from (b) and (d).

TABLE I. The root-mean-square thermal amplitude perpendicular to the surface $[(\Delta z)^2]^{1/2}$, the critical impact angle Ψ_c, the surface lattice constant a, the relative number of vacancies n in the two top layer [1$\bar{1}$0] chains, and the mean-square displacement q between the experimental and the calculated I vs Ψ distributions for three temperatures.

	T (K)		
	160	276	395
$[(\Delta z)^2]^{1/2}$ (Å)	0.207	0.271	0.324
$\Psi_{c,[1\bar{1}0]}$ (deg)	22.70	22.06	21.18
$\Psi_{c,[1\bar{1}2]}$ (deg)	14.66	14.66	14.66
$a_{[1\bar{1}2]}$ (Å)	6.06	6.06	6.06
$a_{[1\bar{1}0]}$ (Å)	3.50 ± 0.01	3.63 ± 0.01	3.82 ± 0.01
$n_{[1\bar{1}0]}$ (%)	10.4 ± 2	8.8 ± 2	9.2 ± 2
$n_{[1\bar{1}2]}$ (%)	10.3 ± 2	9.2 ± 3	13.6 ± 4
$q_{[1\bar{1}0]}$ (10^{-5})	6.1	3.2	3.8
$q_{[1\bar{1}2]}$ (10^{-4})	6.2	3.2	2.5

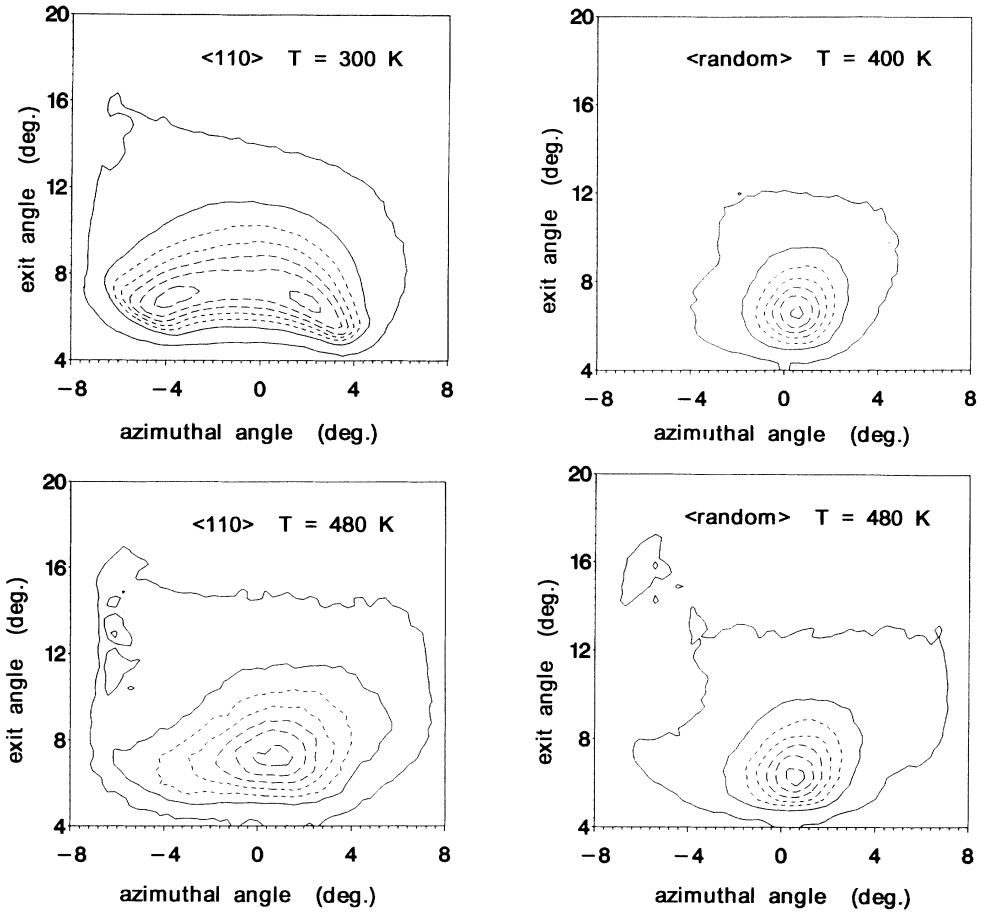

FIG. 3. Surface channeling patterns (2 keV Ne^+), angle of incidence 6° along [1$\bar{1}$0] and [random] (27.5° off [1$\bar{1}$0]) at 300, 400, and 480 K, respectively. The scaling is linear with an intensity increase of 0.14 from line to line.

for the [1$\bar{1}$0] surface channels [15,20,22]. For the random direction the intensity distribution is isotropic. At 480 K, however, the half moon shape starts to vanish for the [1$\bar{1}$0] direction, i.e., a more isotropic intensity distribution is found. It is the combination of enhanced thermal vibrations and the decay of the short-range order which prevents the correlated motion of the ions along the surface needed for channeling [17,20]. Trajectory lengths for channeling at our energies are of the order of 50 Å, i.e., average [1$\bar{1}$0] chain lengths are shorter than about 10 atoms at 480 K [18]. From the point of view of surface channeling the disorder is saturated at 480 K.

The I vs ϕ results (Fig. 1) provide a demonstration of the first-layer melting by a different technique. The conclusions based on the behavior of the intensities of the minima along the low index direction are the following: (i) The step formation along [1$\bar{1}$0] and [1$\bar{1}$2] starts at 270 K which causes the blocking and hence the intensity increase in the other directions. (ii) Around 400 K step or adatom formation is occurring in the other directions as well. These findings agree with the results of MEIS, LEED, and XPD [8,10,11], but our results indicate an additional source for an anisotropic behavior not clearly identified previously [10,11]. The NICISS results (Fig. 2, Table I) show the presence of vacancies at all temperatures, predicted theoretically for Pb [21] and other (110) surfaces [23,24], but not found by MEIS or LEED because these techniques are not sensitive to vacancies. The result of atom diffraction experiments, i.e., the high surface mobility, may be related to the presence of vacancies [25]. The most unexpected and unpredicted result is the anomalous thermal lattice expansion (Table I). This may well be the main source for the previously suggested anisotropies [10,11]. The expansion is certainly a form of premelting, because the atoms move out of their lattice sites. This shift is facilitated by the presence of the vacancies. In fact, the small dependence of the number of vacancies on the temperature indicates filling of vacancies by an expansion of the chains. If a 20-atom long chain expands by one lattice unit at each end, the lengths increase is 10%. The previously suggested decay of the chains at higher temperatures [3] is supported by the channeling results (Fig. 3); we estimate the [1$\bar{1}$0] chain lengths to be below 10 lattice constants.

In summary, point defects and steps play a role in the premelting region of Pb(110), the melting may be initiated by an expansion of the $[1\bar{1}0]$ surface lattice constant, and new and independent evidence is found for the surface melting effect.

We thank J. W. M. Frenken for helpful discussion. Financial support by the Deutsche Forschungsgemeinschaft (DFG) is gratefully acknowledged.

[1] J. W. M. Frenken and J. F. van der Veen, Phys. Rev. Lett. **54**, 134 (1985).
[2] J. F. van der Veen, B. Pluis, and A. W. Denier van der Goon, in *Kinetics of Ordering and Growth at Surfaces*, edited by M. Lagally (Plenum, New York, 1990), p. 343.
[3] A. Pavlovska and E. Bauer, Appl. Phys. A **51**, 172 (1990).
[4] A. W. van der Gon, B. Pluis, R. J. Smith, and J. F. van der Veen, Surf. Sci. **209**, 431 (1989).
[5] J. W. M. Frenken, P. M. J. Maree, and J. F. van der Veen, Phys. Rev. B **34**, 7505 (1986).
[6] B. Pluis, T. N. Taylor, D. Frenkel, and J. F. van der Veen, Phys. Rev. B **40**, 1353 (1989).
[7] H.-N. Yang, T.-M. Lu, and G. C. Wang, Phys. Rev. Lett. **63**, 1621 (1989).
[8] K. C. Prince, U. Breuer, and H. P. Bonzel, Phys. Rev. Lett. **60**, 1146 (1988).
[9] R. Lipowsky, U. Breuer, K. C. Prince, and H. P. Bonzel, Phys. Rev. Lett. **62**, 913 (1989).
[10] U. Breuer, O. Knauff, and H. Bonzel, J. Vac. Sci. Technol. A **8**, 2489 (1990).
[11] A. W. D. van der Gon, H. M. van Pinxteren, J. W. M. Frenken, and J. F. van der Veen, Surf. Sci. **244**, 259 (1991).
[12] W. Heiland, Vacuum **39**, 367 (1989).
[13] H. Niehus, Surf. Sci. **145**, 407 (1984).
[14] H. Derks, W. Hetterich, E. van de Riet, H. Niehus, and W. Heiland, Nucl. Instrum. Methods Phys. Res., Sect. B **48**, 315 (1990).
[15] A. Niehof and W. Heiland, Nucl. Instrum. Methods Phys. Res., Sect. B **48**, 306 (1990).
[16] J. Möller, W. Heiland, K. J. Snowdon, and H. Niehus, Surf. Sci. **178**, 475 (1986).
[17] S. Speller, A. Niehof, and M. Schleberger (to be published).
[18] J. K. Gimzewski, R. Berndt, and R. R. Schittler, Surf. Sci. **247**, 327 (1991).
[19] E. van de Riet, H. Derks, and W. Heiland, Surf. Sci. **234**, 53 (1990).
[20] J. Lindhard, Mat.-Fys. Medd. K. Dan. Vidensk. Selsk. **34**, No. 14 (1964).
[21] P. Tibbits, M. Karimi, and D. Ila, J. Vac. Sci. Technol. A **9**, 1937 (1991).
[22] R. Schiffner, G. Goltz, and C. Varelas, Vak. Tech. **26**, 3 (1977).
[23] P. Stoltze, J. K. Nørskov, and U. Landmann, Phys. Rev. Lett. **61**, 440 (1988).
[24] L. D. Roelofs, S. M. Foiles. M. S. Daw, and M. I. Baskes, Surf. Sci. **234**, 63 (1990).
[25] J. M. Frenken, J. P. Toennies, and Ch. Wöll, Phys. Rev. Lett. **60**, 172 (1988).